International Journal of Mechanical and Production Engineering Research and Development (IJMPERD)
ISSN (P): 2249-6890; ISSN (E): 2249-8001
Vol. 8, Issue 4, Aug 2018, 237-246
© TJPRC Pvt. Ltd.

TRANS STELLAR
•Journal Publications •Research Consultancy

EXPERIMENTAL INVESTIGATION OF PFTIG WELDING PROCESS ON 15CDV6 STEEL USING NANOPOWDERS

SKARIYA. P. D[1], SATHEESH. M[2], EDWIN RAJA DHAS[3] & SUNEESH. E[4]

[1,2]*Department of Mechanical Engineering, Noorul Islam Centre for Higher Education, Tamil Nadu, India*

[3]*Department of Automobile Engineering, Noorul Islam Centre for Higher Education, Tamil Nadu, India*

[4]*Department of Production Engineering, Vidya Academy of Science & Technology, Kerala, India*

ABSTRACT

This study investigates the effect of various nanopowders on PFTIG (Powdered flux Tungsten inert gas) welding of HSLA steel. The High strength low alloy (HSLA) steel identified for this work is 15CDV6 steel. Three different nano-oxide powders such as Cr_20_3, ZnO, and NiO were used in this research. The bead geometry analyzed by using various nanopowders and found that NiO flux has a remarkable effect on penetration and aspect ratio, whereas Cr_20_3 flux was unfavorable in this study. The results indicate that 15CDV6 steel welds pasted with NiO nano flux reduce the risk of solidification cracking susceptibility (SCS). The presence of reversal of Marangoni convection found in the dissolved oxygen concentration results using NiO and ZnO nano fluxes and exceeds the required range of 70 ppm. The arc voltage values using NiO flux pointed to higher heat input, and peak temperatures result in welding arc contraction. The Cr_20_3 nano flux provides a poor bead geometry compared to conventional TIG welding and other powders.

KEYWORDS: PFTIG Welding, HSLA Steel, Bead Geometry & Nano Flux

Received: May 17, 2018; **Accepted**: Jun 07, 2018; **Published**: Jul 04, 2018; **Paper Id**: IJMPERDAUG201826

Original Article

1. INTRODUCTION

15CDV6is low carbon steel belongs to HSLA family [1]. It is a French designation and chromium denoted as C, molybdenum as D and vanadium as V [2]. The steel has excellent weld ability hence the carbon content is 0.15%[3]. It finds its applications in rocket motor casings, pressure vessels etc. [4]. Tungsten inert gas welding is the widely accepted process for joining High strength low alloy steels, as it can generate an excellent and defect-free weld [5]. The multiple pass TIG welding using filler wire is generally used for the fabrication of this type of steels [6]. Due to multiple pass TIG welding, the uneven thermal cycles lead to the non-uniformity of residual stresses and promote the risk of solidification cracking susceptibility (SCS) [7]. This limitation can be covered by using powdered flux TIG welding using nanopowders. The single pass TIG welding using nanopowders reduces the chances of uneven thermal cycles and provides the desired bead geometry. The powdered flux TIG or PFTIG welding thereby reduces the risk of hot cracking tendency. PFTIG welding provides an economical and commercial way of escalating the deeper diffusion of heavy alloy welds [8]. PFTIG welding provides a better joint penetration, thus escalating the efficiency of GTAW to finish thicker welds with the help of reduction in no of passes [9]. The nanopowders decompose easily due to its lower particle size and lower thermal stability compared to micro powders [10]. It will provide the desired bead geometry and macrostructure in HSLA steels.

In PFTIG welding process, a flux is applied before the area to be welded, and it is a mixture of well size

particle of strong oxidizing agents [11]. In general, the nano flux used in PFTIG process results in a deeper penetration as it can generate a centripetal flow of weld metal, high-temperature gradient, and slender arc. The attractive features of PFTIG welding include the reduction in angular distortion and conversion of tensile to compressive residual stress followed by welding in HSLA alloy welds [12]. Kuang-Hung Tseng et al., [13] reported that the oxide fluxes having low thermal stability, such as MoO_3 and Cr_20_3 is providing a better bead geometry compared to the oxides having high thermal stability such as Al_2O_3, MgO, and CaO. Surinder Tathgir et al., [14] conducted a study using various flux powders, i.e.SiO_2, MoO_3, MoS_2, CrO_3, and $TiO_2$and they promote the depth of penetration effectively and in some situations penetration ahead of plate thickness is achieved in alloy and duplex stainless steels. G Chandrasekar et al., [15] investigated a study using flux powders such as TiO_2, $SiO_2$and a mixed component of these fluxes on bead morphology, mechanical properties and microstructure study on Inconel 600. They concluded that the mixed proportion of fluxes (50 % TiO_2 and 50% SiO_2) enhances the optimum bead geometry and the desired DWR obtained while applying this proportion. Srirangan Arun Kumar et al., [16] conducted a study regarding various fluxes such as SiO_2, ZnO, and 50% ZnO and 50% SiO_2in the form of nanopowders and welded with similar settings and factors. The mechanical and metallurgical characteristics were studied and found SiO_2nanopowder provided a deeper penetration, but ZnO powder was unfavorable to the bead geometry. Xiong Xie et al., [17] reported that nanopowders in TIG welding enhance a deeper penetration and a narrower bead width due to its effective dissociation and the heat input procured from the ATIG welding process.

It is identified that no studies have been conducted while considering the literature regarding the development of nanopowders for PFTIG welding of 15CDV6 HSLA steels. This research has been conducted to seek the excellent nano flux for the fabrication of 15CDV6 steel joints. In this paper, the effect of nanopowders on the bead morphology of HSLA steel welds and its impact on arc voltage, heat input, and peak temperature was also presented. The dissolved oxygen concentration and joint penetration ability using nanopowders have also been studied for investigating the mechanism behind the desired bead geometry. The solidification cracking susceptibility test has also been carried out for understanding the effect of nano fluxes on total crack length in PFTIG welded HSLA steel. The outcome of this research is extremely useful to the manufacturing and fabrication sectors that are using 15CDV6 steel.

2. EXPERIMENTAL DETAILS

The 15CDV6 steel of dimensions 1000 x 650 x 6.2 mm was procured from Liquid propulsion systems center, Thiruvananthapuram, Kerala. The 6.2 mm thick plates sliced into 100mm x 100mm strips and make a contaminant-free plate with the help of acetone. Table 1 shows the chemical content of 15CDV6 steel. The single-pass TIG welding is used to make the bead-on-plate welds with an autogenous setup. The process parameters are listed in table 2. Three types of activated nano fluxes such as Cr_20_3, ZnO, and NiO is used for the work. The Ellingham diagram showing the Gibbs free energies of formation of various oxides is mentioned in figure 1. It can be seen that the Gibbs free energies of Cr_20_3, ZnO, and NiO are lower than other oxides. The selected nano oxides featured a relatively low thermal stability to dissociate at high-temperature than other oxides. The oxide fluxes with a nano-size of 40–60 nm and it was procured from ultra nano labs, Gurgaon, Haryana. For making a paste, the methanol is combined with the nanopowder sand a brush of width 10 mm used during welding. The flux-to-methanol ratio has been managed at 1:6.5. Kemppi master GTAW welding machine with the automated setup is used in this work, and the diagram of PFTIG welding process is illustrated in figure 2.

Table 1: Chemical Content of 15CDV6 Steel

Element	C	Cr	Mn	Mo	Ni	V	Si	Cu	P
Weight %	0.152	1.229	0.838	0.791	0.234	0.198	0.189	0.107	0.005

After welding, the bead on plate specimens was sectioned transversely, polished and etched using standard procedures before subjecting to the macro graphic study. The etchant used in this study is glyceregia. In this study, the optical microscope provides the macrostructure of the bead geometry, and the dimensions ie DOP, BW and HAZ width were measured with the help of image J software. The solidification cracking tendency was assessed with the assistance of avarestraint test machine. The 80A current, arc time7s and the arc length of 1.6mmwere considered as factors for welding 3-mm-thick 15CDV6 alloy plate. A 5% tangential strain is transmitted to the top part of the specimen.

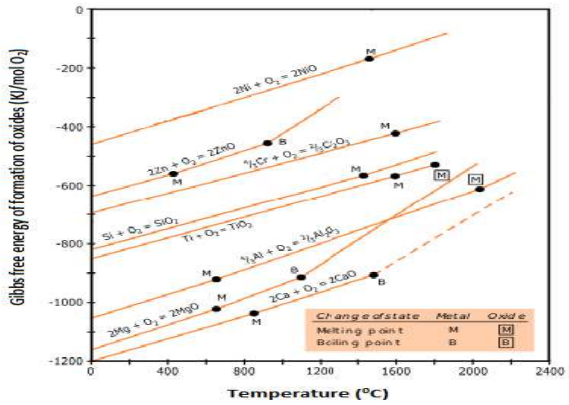

Figure 1: Ellingham Diagram for Selected and Other Oxides

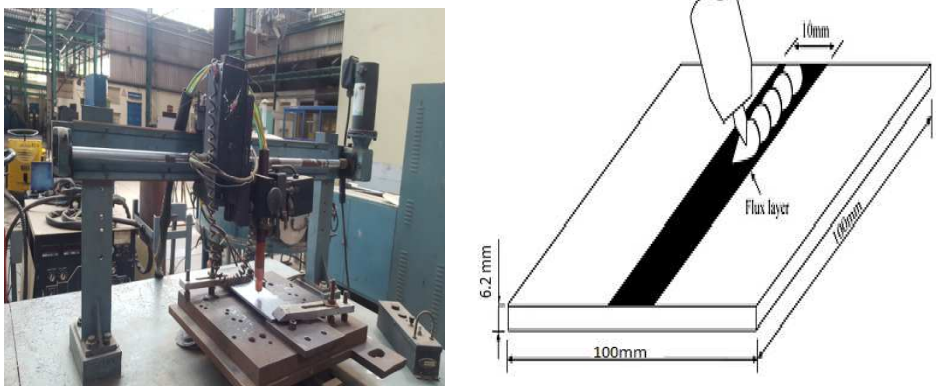

Figure 2: Kemppi Master TIG 4000 Welding Machine and Schematic Diagram of PFTIG Welding

The welding trials were performed to measure the peak temperature with the support of a ‘‘K’’ type contact-thermocouple. The oxygen concentrations in the weld were measured with the assistance of an O_2analyser. The arc voltage measured from the display of the welding equipment itself.

Table 2 Welding Parameters for Initial Experiments

Welding current	180 Amperes	**Torch angle**	110 degree
Travel speed	78 mm/min	**Gas flow rate**	8 ltr/min
Arc gap	1.5 mm	**Diameter of electrode**	3.2 mm

3. RESULTS AND DISCUSSIONS

3.1. Effect of Nano Fluxes on Bead Geometry

The macrostructure of various weld-bead profiles is illustrated in figure 3. The Cr_20_3 flux and autogenous GTAW welding exhibited a low penetration of 3.047 mm and 3.187 mm, but ZnO and NiO nano fluxes produced a deeper penetration of 4.371 and 4.743 mm. The NiO nano powder in PFTIG welding exhibited a deeper penetration and narrower bead width compared to all other powders and conventional TIG welding process. The dimensions obtained from the macrostructure ie DOP (depth of penetration), BW (bead width), HAZ (heat affected zone) width and DWR is shown in table 3.

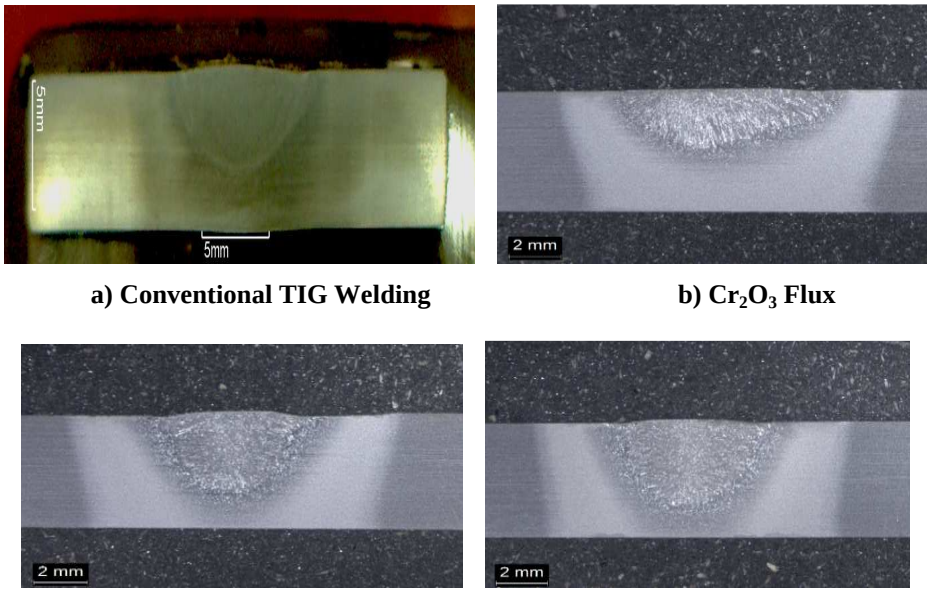

a) Conventional TIG Welding **b) Cr_2O_3 Flux**

c) ZnO Flux **d) NiO Flux**

Figure 3: Transverse Cross-Section of TIG Welds with and Without Nano Powdered Oxides

Table 3: Bead Geometry from Macrostructure for with and without Nano Fluxes

Nano Flux	Depth of Penetration (mm)	Bead width (mm)	HAZ Width (mm)	Depth to Width Ratio (DWR)
Normal TIG/No flux	3.187	9.336	2.848	0.341
Cr_20_3	3.047	6.849	2.749	0.445
ZnO	4.371	5.876	2.636	0.744
NiO	4.743	5.497	2.489	0.863

The penetration capacity of PFTIG welds was larger than conventional TIG weld and Cr_20_3 flux. The increased DOP and narrower BW were due to the escalated oxygen content, which can be substantiated using the phenomenon of reversal of Marangoni convection [18]. This theory stated that surface tension gradient increase with a rise in temperature [19]. The peak temperature portion, ie the molten pool pulls the fluid from the surrounding area, and an outward to inward flow was found to be occurring. This phenomenon resulted in a narrower bead width. This theory was strongly supported by the fact that the presence of surface active elements, i.e oxygen, sulfur etc. in the molten pool and it was discussed in this paper later. As shown in figure 1, Ellingham diagram points out that Nickel oxide has lower thermal stability out of all the oxides and this property leads to the dissociation of more oxygen, which in turn promotes the reversal of Marangoni flow and results in deeper penetration. The lower DOP was due to the inefficient synergy between the chemical content of

the base material and the used nanopowder that cannot establish a Marangoni flow.

The depth to width ratio or DWR is DOP divided by BW. The higher value of DWR or aspect ratio is the indication of an optimum weld bead [20]. The aspect ratio was found to be lower in the case of normal TIG and Cr_20_3 flux due to its shallower penetration, whereas ZnO and NiO nanopowders showed a deeper penetration and resulted in a higher DWR.

3.2. Effect of Nano Fluxes on Joint Penetration Ability and Oxygen Concentration

The Joint penetration ability (JPA)of TIG welds obtained with the presence and absence of oxides is shown in figure 4. The JPA of the weld [13] is characterized by the % variation in the weld depth (%ΔD), that can be expressed as:

$\%\Delta D = (D_W - D_{W/O})/ D_{W/O} \times 100\%$

The depth of the weld obtained in the presence of oxide is $D_w$and in the absence of oxide is $D_{w/o}$ The ZnO and NiO powders enhance the Joint penetration ability of 15CDV6 steel TIG welds while comparing with Cr_20_3flux.

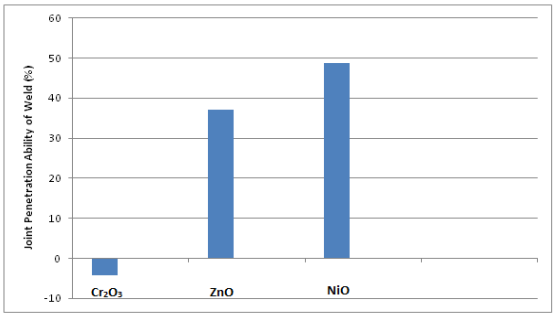

Figure 4: Joint Penetration Ability of TIG Welds Produced with Nano Powdered Oxides

The dissolved oxygen concentration (DOC) in TIG welds procured in the presence and absence of oxides is illustrated in Table 4. The results indicate that DOC in 15CDV6 steel normal TIG weld was 39 ppm. ZnO and NiO nano fluxes have DOC of 73 and 78 ppm. The DOC obtained while using Cr_20_3 flux was 34 ppm, and the concentration is very low as compared to normal TIG welding. This study can conclude that necessary oxygen content present in the molten pool obtained with ZnO and NiO and thus the Marangoni flow changes from centrifugal to centripetal flow. The higher oxygen concentration was also attributed to the lower Gibbs free energy formation of these oxides as shown in figure 1. TheCr_20_3 flux and normal TIG welding indicate the deficient oxygen content in the molten pool. The dissolved oxygen concentration and presence/absence of reversed Marangoni mechanism are shown in table 4. The lower DOC of Cr_20_3 flux and normal TIG welding was attributed to the absence of Marangoni flow reversal in these weldments and leads to the shallow penetration and wider bead geometry. The Marangoni flow reversal occurs only when the dissolved oxygen concentration of surface active elements ranges from 70 to 300 ppm [21]. The DOC obtained for ZnO, and NiO nano fluxes were greater than 70 ppm. The Cr_20_3 nano flux is not completely dissociated in the pool to produce necessary oxygen in 15CDV6 steel. The experimental results have proven that the DOC of ZnO and NiO enhances the reversal of Marangoni mechanism in these two weldments and leads to the bead geometry having deeper penetration and narrower bead width.

Table 4 Effect of with and without Nano-Oxide Fluxes on DOC and Reversal of Marangoni Effect

Nano Flux	Dissolved Oxygen Concentration (ppm)	Reversal of Marangoni Effect
Normal TIG/No flux	39	Absent
Cr_20_3	34	Absent
ZnO	73	Present
NiO	78	Present

3.3 Effect of Nano Fluxes on Arc voltage, Heat Input, and Peak Temperatures

The nano fluxes enhance the voltage of the arc, and it is due to the presence of ionization potential in the arc gap. The fluxes used in this study are having a different chemical composition, and the variations in the voltage were recorded. Furthermore, the dissociated flux at peak welding temperatures generates positive ions, and at the same time, the arc contained numerous free electrons. These dissociated fluxes captivate the free electrons, resulting in the constriction of the welding arc [22]. It has been already proven that welding arc tends to contract when the voltage within the arc was increased. The use of ZnO and NiO fluxes escalates the arc voltage by 2 V when compared to Cr_2O_3 and normal TIG welding.

The voltage of the arc measured and the calculated heat input was mentioned in table 5andobserved that PFTIG welding increases the values of the heat input which leads to the increment of the peak temperature values. The maximum acceptable heat input for this category of steel is 2 KJ/mm [23]. The excessive heat input provides a coarse grain structure, and it has a negative impact on mechanical properties. From table 5, it is clear that the heat input values are within the limit. The arc contraction increases the heat of the specimen results in the increment of current per unit area and hikes in peak temperatures while using PFTIG welding [24]. This increase in current density followed by arc contraction escalates the DOP and reduces the BW [25]. Thetable5 indicates that the peak temperature rises while using nano fluxes such as ZnO and NiO and hence the maximum penetration has been obtained with the consumption of these two fluxes. The peak temperatures were found to be very low in the case of Cr_2O_3, and normal TIG welding and these results were attributed to the matter that the arc was not contracted in these welds.

Table 5: Effect of with and Without Nano-Oxide Fluxes on the arc Voltage, Heat Input and Peak Temperatures

Nano Flux	Arc voltage (V)	Heat input (KJ/mm)	Peak Temperature (^{0}C)	Arc constriction Mechanism
Normal TIG/No flux	14.3	1.39	618	Absent
Cr_20_3	14.1	1.37	577	Absent
ZnO	15.8	1.53	738	Present
NiO	16.3	1.58	841	Present

3.4 Effect of Nano Fluxes on Solidification Cracking Susceptibility (SCS) of Weldments

The crack morphology of the 15CDV6 HSLA steel welds tested with the help of restraint test is shown in figure5. The resistance of solidification cracking in PFTIG welding is larger than normal TIG welding. The heat input highly influences solidification cracking, implies that cracking susceptibility reduces with an increase in energy density [7, 26].

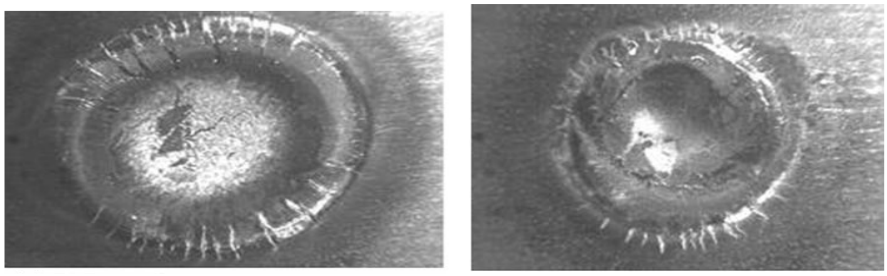

a) Without Nano Flux
Total crack length = 38.06 mm

b) Cr_2O_3 Nano Flux
Total crack length = 33.07 mm

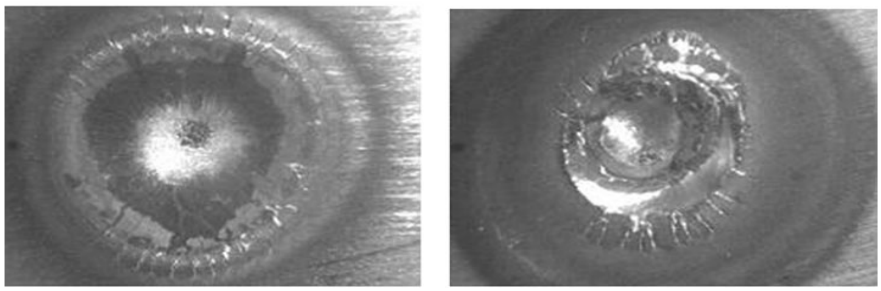

c) ZnO Nano Flux
Total crack length = 17.86 mm

d) NiO Nano Flux
Total crack length = 12.32 mm

Figure 5 Effect of with and without Nano Fluxes on Solidification Cracking Susceptibility

The deeper penetration can be obtained in PFTIG welds due to larger current and heat density, and thus the activating fluxes reduce the solidification cracking tendency of 15CDV6 alloy welds. The figure 5 reveals that normal TIG welding and Cr_2O_3 nano flux have no significant effect in reducing the total cracking length or solidification cracking susceptibility of 15CDV6 steel weldments. The PFTIG welding using ZnO and NiO nano fluxes reduces the cracking tendency, and it was proven from the total crack length acquired while using these fluxes. The total crack length was found to be 17.86 and 12.32 mm respectively, with the consumption of these fluxes. NiO and ZnO fluxes are having a higher energy density while PFTIG welding and it was attributed to its higher arc voltage and arc constriction mechanism. From the results, it came to conclude that solidification cracking susceptibility of 15CDV6 steel welds can be reduced with the use of NiO and ZnO nano fluxes.

4. CONCLUSIONS

The current research work stated the successful welding of 15CDV6 HSLA Steel by PFTIG welding using nanopowders. The significant outcomes from this research work are mentioned below:

- The NiO flux gives the maximum penetration in 6.2 mm15CDV6 steel bead on plate weld. PFTIG welding factors were strongly utilized to weld HSLA steel in a single pass autogenous TIG welding.
- PFTIG welding using Cr_2O_3 nano flux and normal TIG welding has no significant effect on DOP and DWR.
- The oxygen concentration in ZnO and NiO weld beads exceeds the standard limit of 70 ppm, whereas the presence of reversal of Marangoni convection has occurred.
- The arc voltage was found to be high using NiO flux which leads to larger heat input and peak temperatures and results in the constriction of the arc.

- The total crack length was found to be lower in solidification cracking susceptibility (SCS) test while using NiO and ZnO nano fluxes.

REFERENCES

1. *Bandyopadhyay, T. R., Rao, P. K. and Prabhu, N., 2012. Improvement in mechanical properties of standard 15CDV6 Steel by increasing carbon and chromium content and inoculation with Titanium during ESR. ISRN Materials Science, 2012, 1-7 Article ID 572703. doi: 10.5402/2012/572703*
2. *Kumar, P. N., Bhaskar, Y., Mastanaiah, P. and Murthy, C.V.S., 2014. Study on dissimilar metals welding of 15CDV6 and SAE 4130 steels by inter pulse gas tungsten arc welding. Procedia Materials Science, 5, pp.2382-2391.*
3. *Srinivasan, L., Kannan, T.D.B., Sathiya, P. and Biju, S., 2017. Effect of heat input, heat treatment on microstructure and mechanical properties of GTA welded aerospace material 15CDV6. Journal of Materials Research, 32(7), pp.1361-1366.*
4. *B V R Ravi Kumar and J S Soni, Microstructure and properties of welded 15CDV6 alloy steel. ICFAI J. Sci. Technol.5, 1–19 (2009).*
5. *Bhole, S.D. and Fox, A.G., 1996. Influence of GTA welding thermal cycles on HSLA-100 steel plate. Canadian metallurgical quarterly, 35(2), pp.151-158.*
6. *Emamian, A., Emamian, A. and Kowkabi, A.H., 2010. Effects of filler wire composition along with different pre-and post-heat treatment on mechanical properties of AISI 4130 welded by the GTAW process. Materials Sciences and Applications, 1(03), p.135.*
7. *Shyu, S.W., Huang, H.Y., Tseng, K.H. and Chou, C.P., 2008. Study of the performance of stainless steel A-TIG welds. Journal of Materials Engineering and Performance, 17(2), pp.193-201.*
8. *Tseng, K.H. and Hsu, C.Y., 2011. Performance of activated TIG process in austenitic stainless steel welds. Journal of Materials Processing Technology, 211(3), pp.503-512.*
9. *Tathgir, S., Bhattacharya, A. and Bera, T.K., 2015. Influence of current and shielding gas in TiO2 flux activated TIG welding on different graded steels. Materials and Manufacturing Processes, 30(9), pp.1115-1123.*
10. *Tseng, K.H. and Lin, P.Y., 2014. UNS S31603 stainless steel tungsten inert gas welds made with microparticle and nanoparticle oxides. Materials, 7(6), pp.4755-4772.*
11. *Modenesi, P.J., Apolinario, E.R. and Pereira, I.M., 2000. TIG welding with single-component fluxes. Journal of materials processing technology, 99(1), pp.260-265.*
12. *Dhandha, K.H. and Badheka, V.J., 2015. Effect of activating fluxes on weld bead morphology of P91 steel bead-on-plate welds by flux assisted tungsten inert gas welding process. Journal of Manufacturing Processes, 17, pp.48-57.*
13. *Tseng, K.H. and Shiu, Y.J., 2015. Effect of thermal stability of powdered oxide on joint penetration and metallurgical feature of AISI 4130 steel TIG weldment. Powder Technology, 286, pp.31-38.*
14. *Mohammed, Samir, Ata El-Kareim Shoeib, and Mostafa Abd El-Megied. "Effect of Discrete Steel Fibers on the Behaviour of RC Beams Exposed to Fire."*
15. *Tathgir, S. and Bhattacharya, A., 2016. Activated-TIG welding of different steels: influence of various flux and shielding gas. Materials and Manufacturing Processes, 31(3), pp.335-342.*
16. *Chandrasekar, G., Kailasanathan, C. and Verma, D.K., 2017. Investigation on un-peened and laser shock peened weldment of Inconel 600 fabricated by ATIG welding process. Materials Science and Engineering: A, 690, pp.405-417.*

17. *Kumar, S.A. and Sathiya, P., 2015. Experimental investigation of the A-TIG welding process of Incoloy 800H. Materials and Manufacturing Processes, 30(9), pp.1154-1159.*

18. *Xie, X., Shen, J., Cheng, L., Li, Y. and Pu, Y., 2015. Effects of nano-particles strengthening activating flux on the microstructures and mechanical properties of TIG welded AZ31 magnesium alloy joints. Materials & Design, 81, pp.31-38.*

19. *Tseng, K.H. and Chuang, K.J., 2012. Application of iron-based powders in tungsten inert gas welding for 17Cr–10Ni–2Mo alloys. Powder technology, 228, pp.36-46.*

20. *Paskell, T., Lundin, C. and Castner, H., 1997. GTAW flux increases weld joint penetration. Welding Journal, 76(4), pp.57-62.*

21. *Yang, C.L., Lin, S.B., Liu, F.Y., Wu, L. and Zhang, Q., 2003. Research on the mechanism of penetration increase by flux in A-TIG welding. J. Mater. Sci. Technol, 19(1), pp.225-227.*

22. *Singh, Shiv Sagar, and Abhishek Gaikwad. "Comparison of Mechanical Properties of Dual Phase Steel for Different Quenching Mediums."*

23. *Vasudevan, M., 2017. Effect of A-TIG Welding Process on the Weld Attributes of Type 304LN and 316LN Stainless Steels. Journal of Materials Engineering and Performance, 26(3), pp.1325-1336.*

24. *Vora, J.J. and Badheka, V.J., 2015. Experimental investigation on mechanism and weld morphology of activated TIG welded bead-on-plate weldments of RAFM steel using oxide fluxes. Journal of Manufacturing Processes, 20, pp.224-233.*

25. *Srinivasan, L., Jakka, S.J. and Sathiya, P., 2017. Microstructure and mechanical properties of Gas tungsten arc welded High Strength Low Alloy (15CDV6) steel joints. Materials Today: Proceedings, 4(8), pp.8874-8882.*

26. *C.R. Heiple, J.R. Roper, Mechanism for minor element effect on GTA fusion zone geometry, Weld. J. 61 (1982) 97–102.*

27. *Vora, J.J. and Badheka, V.J., 2016. Improved penetration with the use of oxide fluxes in activated TIG welding of low activation ferritic/martensitic steel. Transactions of the Indian Institute of Metals, 69(9), pp.1755-1764.*

28. *Lin, H.L., Wu, T.M. and Cheng, C.M., 2014. Effects of flux precoating and process parameter on welding performance of Inconel 718 alloy TIG welds. Journal of materials engineering and performance, 23(1), pp.125-132.*